Al-Azhar University Civil Engineering Research Magazine (CERM)
Vol. (41) No. (3) July, 2019

ULTIMATE CAPACITY OF STEEL SHEAR WALLS WITH CORRUGATED PLATE

Abdelrahim K. Dessouki[1], Sherif A. Ibrahim, P.E. [2], Ibrahim N. N. Shenouda [3]

1-Professor, Structural Engineering Department, Ain Shams University, Cairo, Egypt,
2- Professor, Structural Engineering Department, Ain Shams University, Cairo, Egypt,
3-Research student, Structural Engineering Department, Ain Shams University, Cairo, Egypt.

ملخص البحث.

هذه الرسالة تدرس المقاومة القصوي لحوائط القص المعدنية ذات الألواح المعرجة. تم إنشاء نماذج ثلاثية الأبعاد باستخدام برنامج ABAQUS بطريقة العناصر المحددة. تعتبر حوائط القص من الانظمه المستخدمه حديثا في مقاومة الاحمال العرضيه. لدراسة المقاومه القصوي لحوائط القص ذات الألواح المعرجه تم اولا دراسة مقاومة حوائط القص المعدنيه ذات الألواح المستويه ثم مقارنة مقاومته القصوي مع حوائط القص المعدنيه ذات الألواح المعرجه. تم دراسة الحوائط المعدنيه ذا الألواح المعرجه ذات القطاع شبه منحرف واخري ذات القطاع علي شكل قطع ناقص. تم ايضا دراسة حوائط القص المعرجه ذات الاتجاهات الافقيه والراسيه والمائله من حيث إتجاه الالواح المعدنيه. قد وجد ان حوائط القص المعدنيه ذات الالواح المعرجه علي شكل شبه منحرف والموجه بها الألواح المعدنيه بصوره رأسيه لها مقاومه قصوي أعلي من باقي الحوائط المعدنيه نظيرتها من حيث توجه شكل الالواح المعرجه وذلك لان تلك الحوائط لها ثبات في التشكل علي المستوي العمودي علي الحائط. ايضًا تم الإهتمام بتحديث المعادلات اللتي تدرس مقاومة الالواح المعرجه للاجهادات الناتجه عن الانبعاج الحادث بها.

Abstract.

Steel shear walls with corrugated plates (SSWCP) is a new widely used technique to resist the lateral forces in the high-rise buildings. Ultimate capacity of the SSWCP is investigated in this research using finite element models and comparison with flat plate shear walls is achieved. Three-dimensional models using shell elements for both infill plate and boundary frame are used. Several geometrical parameters control the results such as infill plate thickness, corrugation density, corrugation dimensions, corrugation orientation and boundary frame geometrical properties. Using corrugated steel plate in shear walls affects directly the shear wall capacity. Corrugated plate shear walls not necessarily have higher ultimate capacity more than flat shear walls. Vertically oriented corrugated shear walls have higher capacity than other orientations but it may have less stiffness compared with the inclined corrugated shear walls. Changing the orientation of the corrugation affects the ultimate bearing capacity of the shear wall. It is found that trapezoidal corrugated infill plate has better performance than the sinusoidal corrugated infill plate as well as less cost and weight. Updating the critical buckling stress formula for trapezoidal corrugated shear walls taking into consideration several parameters is included in this research.

Keywords: Steel shear wall; Corrugated plates; Finite elements; Local buckling; Global buckling; Interactive buckling; Tension field action; Boundary frame.

1- Introduction

Lateral force is one of the most important straining actions in the design of multistory buildings. The system that resists this force must be economically designed. Several systems are used to resist lateral loads such as moment frames, braced frames

and shear walls. Steel shear walls were previously used in several buildings to resist the lateral load; and especially those with corrugated infill plates. The out of plane stability of the shear wall generally and especially those for the corrugated infill plate gives a great advantage for the shear wall compared with moment frames when it is subjected to lateral loads. The failure may be caused generally by diagonal tension field action. As the infill plates are usually thin plates, the total weight of the shear walls are always lighter than moment frames.

Corrugated plates are used as infill plate for the shear wall as it has relatively higher stability in the out of plane direction compared with flat plates. The failure of the infill plate is converted from diagonal tension field action in the flat infill plate to corresponding local and global buckling in the corrugated plate. The type of failure generally depends on the main component of the shear wall (Vertical boundary element "VBE", Horizontal boundary element "HBE" and infill plate). Figure 1 represents the main components of the steel plate shear walls used in this study.

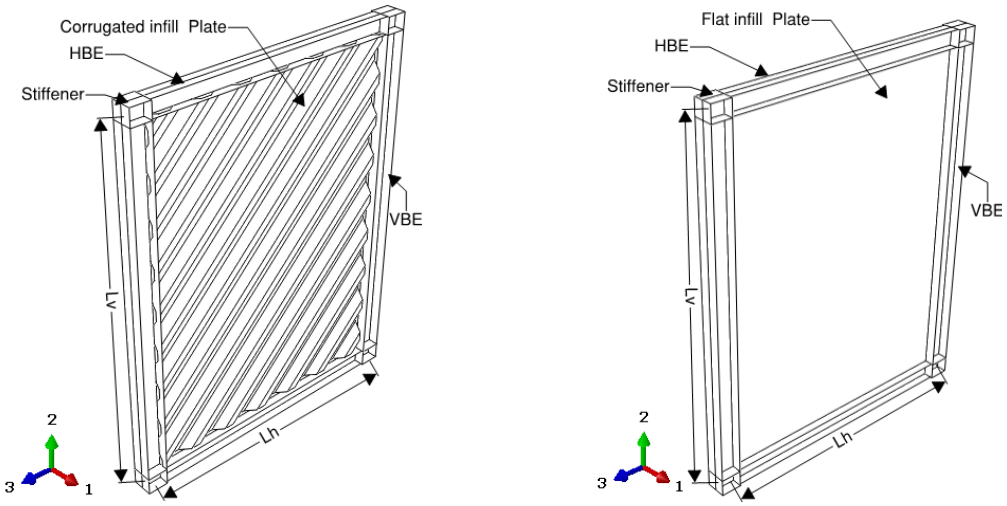

Figure 1 Typical shear wall layout with corrugated web and flat infill plate

2- Theoretical background

2.1. Flat infill steel shear plates

Thorburn, et al. [1] proposed the first equation to represent the diagonal tension angle (β^0) for plates through Equation (1). They used the strip model to get this equation where the infill plates are replaced by a series of inclined tension strips.

$$\tan^4\beta = \frac{1 + \left(L.t_p / 2.A_c\right)}{1 + \left(H.t_p / A_b\right)} \qquad (1)$$

Timler et al. [2], revised equation (1) to include the effects of column flexibility as indicated in equation (2), where; L is the frame bay width, H is the frame story height, t_p is the panel thickness, and A_b and A_c are gross cross-sectional areas of the story beam and column, respectively. I_c is the moment inertia of boundary column.

$$\tan^4\beta = \frac{1 + \left({}^{L.\,t_p}/_{2.\,A_c}\right)}{1 + Ht_p\left[{}^{1}/_{A_b} + {}^{H^3}/_{360.\,L.\,I_c}\right]} \quad (2)$$

Berman et al., [3] used equilibrium and kinematic methods of plastic analysis, that assumed collapse mechanism for the strip model to produce an expression for single story shear wall ultimate strength. The method is identical to that of the CAN/CSA S16-01 procedure, which is used in calculating the shear resistance of a steel shear wall with flat infill panel as per equation (3).

$$V_{yp} = \frac{1}{2}.F_{yp}.t_p.L.\sin 2\beta \quad (3)$$

Moreover, B. Qu1 and M. Bruneau2 [4] performed a research on developing capacity procedure for VBEs in SSWPs. They reviewed the current approaches provided in the AISC Seismic Provisions (AISC 2005) for determination of capacity design loads for VBEs of SSWPs and identified the deficiency of these procedures. A new procedure was proposed based on a fundamental plastic collapse mechanism and linear beam analysis to approximate the design actions for VBE for the given infill panel and HBE. It was found that VBE design forces predicted from the proposed procedure agree well with those from the nonlinear pushover analysis. In addition, equation (4) which was based on the plastic analysis was confirmed to represent the overall flat plate shear wall capacity, where M_p is the lowest plastic moment capacity of either VBE or HBE.

$$V_{yp} = \frac{1}{2}.F_{yp}.t.L.\sin 2\beta + 4\frac{M_P}{H} \quad (4)$$

Jalali et al., [5] performed theoretical and experimental post-buckling study on "Steel Shear Walls Plate" SSWPs. A small scale SSWP consisting of 300 mm x 500 mm infill panel and the boundary connection with infill plate is considered as simple connection. The specimens are tested under cyclic loading in order to evaluate the force-displacement relation and post-buckling behavior of the specimen. The drifts corresponding to the yielding and rupture in the panel were 1.7% and 5% respectively.

Figure 2 shows the dimensions and designation of each part of the corrugated shear wall used in this research.

2.2. Corrugated steel plate shear walls

El-Gaaly et al., [6, 7 and 8] studied the trapezoidal corrugated plate buckling behavior when it is used as beam's web. They conducted equation (5) to represent the trapezoidal corrugated plate local buckling stress and equation (6) to represent the trapezoidal corrugated plate global buckling stress.

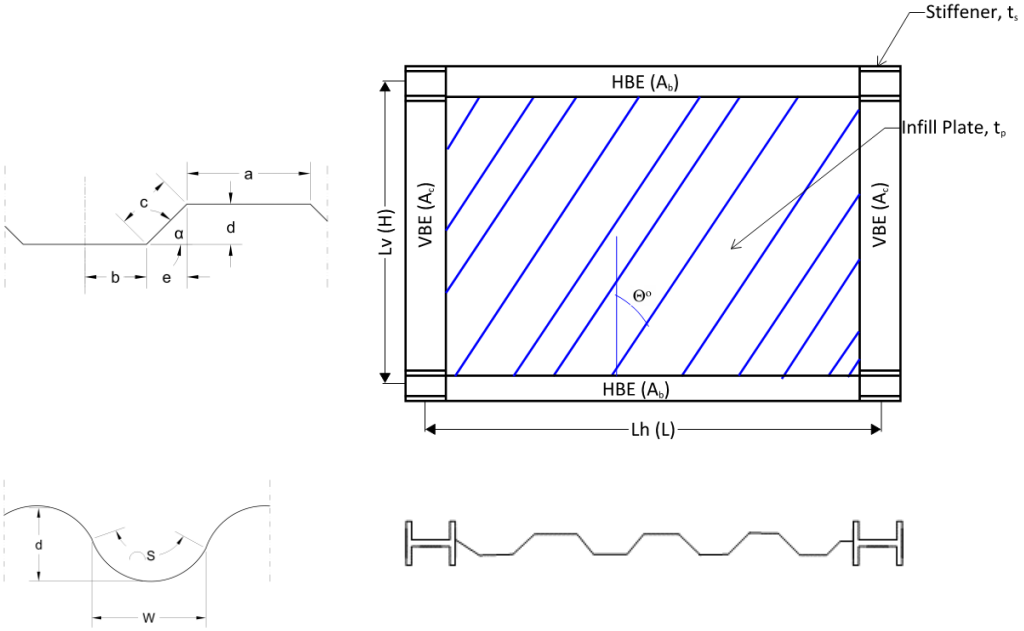

Figure 2 Shear wall sketch with corrugated infill plate data[5]

$$\tau_{crl} = k_l \left[(\pi)^2 \frac{E}{12(1-\nu^2)}\right] . \left[\frac{t_p}{w}\right]^2 \quad (5)$$

$$\tau_{crG} = k_G \left[(\pi)^2 \frac{E}{12(1-\nu^2)}\right] . \left[\frac{t_p}{h_w}\right]^2 \quad (6)$$

Where τ_{crl} is the elastic local shear buckling stress, τ_{crG} is the elastic global shear buckling stress. k_l is the local shear-buckling coefficient as per equation (7). k_G is the global shear-buckling coefficient as per equation (8). E is Young's modulus, ν is Poisson's ratio, w is the maximum fold width (maximum of flat panel width or inclined panel width c), h_w is the web plate straight height and d is the corrugation height.

$$k_l = 5.34 + 4 \left[\frac{h_w}{w}\right]^2 \quad (7)$$

$$k_G = 5.72 \left(\frac{d}{t_p}\right)^{1.5} \quad (8)$$

Berman et al. (2003a, 2005) [9]; conducted quasi-static cyclic testing on three SSWP specimens. These specimens were: flat infill plate, concentric braced frame and 45° oriented trapezoidal corrugated infill plate. The specimens utilized light gauge and cold-formed corrugated steel for the infill panel material. The researchers reported that the corrugated infill panel contributed over 90% to the total initial stiffness for the corrugated specimen. The specimen exhibited unsymmetrical hysteresis loops since tension field action only developed in the direction of the corrugations.

Kiymaz et al., (2010) [10]; defined the corrugated plate local buckling stress $\tau_{l,s}$ and global buckling stress $\tau_{G,s}$ for sinusoidal corrugated plates as per equations (9) and (10) respectively.

$$\tau_{l,s} = k_{l,s} \left[\frac{(\pi)^2 E}{12(1-\nu^2)}\right] . \frac{t_p}{S} \quad (9)$$

$$\tau_{G,s} = K_{G,s} \frac{\sqrt[4]{D_y}\sqrt[4]{D^3{}_x}}{t_p {h_w}^2} \quad (10)$$

Where S is the wave length of the corrugated plate as per figure 2. $K_{l,s}$ is the local buckling frame factor defined as per equation (11) in a sinusoidal corrugated plate. $k_{G,s}$ is 32.4 for simply supported and 60.4 for clamped boundary conditions. The factors D_x and D_y are plate rigidities in the longitudinal, X, and traverse, Y, directions that are given as equations (12) and (13) respectively. I_x as in equation (14) is the second moment of area for one wave length of the corrugated infill plate.

$$k_{l,s} = 5.34 + 4\left(\frac{S\,.\,d}{2\,t_p\,h}\right) \tag{11}$$

$$D_x = \frac{E\,I_x}{W} \tag{12}$$

$$D_y = \frac{E\,{t_p}^3}{12\,(1-\nu^2)}.\frac{W}{S} \tag{13}$$

$$I_x = \frac{d^2\,t_p}{8}.\left[1 - \frac{0.81}{1 + 2.5\left(\frac{d}{4\,w}\right)^2}\right] \tag{14}$$

Emami (2013) [11]; tested three specimens of single-story, single-bay shear walls. The first specimen is an unstiffened steel shear wall. The second specimen has trapezoidal vertical corrugated panel and the third one has a trapezoidal horizontal corrugated steel shear wall. They derived equation (15) to determine the limiting shear elastic displacement for corrugated panels. U_{wcr} is the shear buckling displacement of the corrugated panel, U_{wpb} is the shear displacement of the corrugated panel due to the tension field action where Θ is the angle of corrugation orientation and h_s is the height of the panel.

$$U_{WE} = U_{Wcr} + U_{Wpb} = \frac{\tau_{cr}}{G} + 3.5\frac{\sigma_{ty}}{E}\sin(2\Theta)h_s \tag{15}$$

3- Problem Statement

Previous researches have been carried out to provide a clear formula regarding the corrugated steel plate capacity and studying the plate frame interaction (PFI). The objective of this paper is to get a suitable equation for the corrugated steel plate shear walls and study the effect of several geometrical parameters on the corrugated shear wall ultimate capacity.

4- Finite element modeling

Thirty groups of shear walls with flat and corrugated infill plate are modeled using ABAQUS software ver. 6.10 [12]. Constant dimensions for a single story shear walls are considered, where h = 4500 mm and L = 3500 mm. Six thicknesses are used for the infill plate in each group (9, 7, 6, 4, 2 and 1 mm) respectively. Five sections from CISC manual [13] for HBE were used (W760x220, W760x434, W460x128, W200x52 and W200x27) and five corresponding sections for VBE were used (W690x240, W690x419, W310x143, W250x80 and W250x39). The material properties are considered as shown in Figure 3 and Table 1. The models are built using four-node thin shell elements (S4R5). Shear wall is considered to have a hinged support at base and simple pin supported in the upper intersection of boundary frame to prevent out of plane deformation as per figure 4. Only horizontal loads are considered at the top of the infill plate as concentrated lateral load. No vertical load was considered in this study.

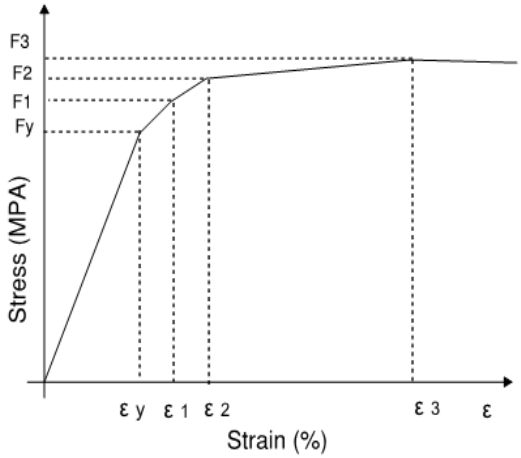

Figure 3 Stress-strain relationship applied to inelastic analysis

	Boundary	Infill Plate	Stiffener
Density (kN/mm^3)	7.85E-09	7.85E-09	7.85E-09
E (MPa)	200000	200000	200000
Poison's	0.3	0.3	0.3
F_y (MPa)	355	310	280
F_1 (MPa)	210	250	200
ε_1	0.1	0.1	0.1
F_2 (MPa)	300	280	250
ε_2	0.15	0.15	0.15
F_3 (MPa)	520	480	420
ε_3	0.2	0.2	0.2

Table 1 Material properties values

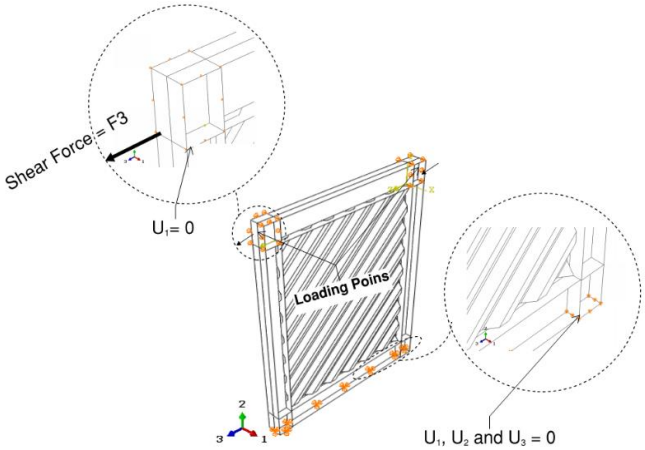

Figure 4 Boundary conditions and loading points for the FE model

Five model groups are developed as guide models for the flat infill plate analysis. Each group has six different models regarding the infill plate thickness. Three groups for each type of the trapezoidal corrugated shear walls are analyzed based on the orientation of the infill plate (Θ^o) (vertical, horizontal, 30^o, 45^o and 60^o). The difference between these groups is the boundary frame properties. Each group has six different models based on the infill plate thickness (while performing the parametric study each thickness is compared with the corresponding one). SSWP FE models are designated as C "Corrugated" and T "Trapezoidal" and then followed by the group number then the specimen number as shown in Table 2.

4.1. Corrugated plate buckling behavior

Mainly, the corrugated infill plates provide and control the shear capacity of frame by their buckling behavior. Plate buckling occurs due to initial imperfection of the plate. Due to load deformation, there are two types of buckling that control the corrugated plates: overall buckling and local buckling. The local buckling mode of corrugated plates is formed in flat panels of trapezoidal corrugated plates according to Figure 5. According to Figure 6, the global buckling is occurred with global diagonal buckling of multi waves in trapezoidal corrugated plate.

Table 2 Geometrical configuration for finite element models

Group No.	HBE	VBE	Corrugation data				Corrugation angle (deg.)
			Deg. (α)	a (mm)	b (mm)	d (mm)	
SSWP-C-T-1	W 200x52	W 250x80	45 °	90	45	90	0 °
SSWP-C-T-2	W 200x27	W 250x39	45 °	90	45	90	0 °
SSWP-C-T-3	W 460x128	W 310x143	45 °	90	45	90	0 °
SSWP-C-T-4	W 200x52	W 250x80	45 °	90	45	90	90 °
SSWP-C-T-5	W 200x27	W 250x39	45 °	90	45	90	90 °
SSWP-C-T-6	W 460x128	W 310x143	45 °	90	45	90	90 °
SSWP-C-T-7	W 200x52	W 250x80	45 °	90	45	90	45 °
SSWP-C-T-8	W 200x27	W 250x39	45 °	90	45	90	45 °
SSWP-C-T-9	W 460x128	W 310x143	45 °	90	45	90	45 °
SSWP-C-T-10	W 200x52	W 250x80	45 °	90	45	90	30 °
SSWP-C-T-11	W 200x27	W 250x39	45 °	90	45	90	30 °
SSWP-C-T-12	W 460x128	W 310x143	45 °	90	45	90	30 °
SSWP-C-T-13	W 460x128	W 310x143	15 °	340	45	90	0 °
SSWP-C-T-14	W 460x128	W 310x143	30 °	155	45	90	0 °
SSWP-C-T-15	W 460x128	W 310x143	60 °	50	45	90	0 °
SSWP-C-T-16	W 460x128	W 310x143	75 °	25	45	90	0 °
SSWP-C-T-17	W 200x52	W 250x80	45 °	90	45	90	60 °
SSWP-C-T-18	W 200x27	W 250x39	45 °	90	45	90	60 °
SSWP-C-T-19	W 460x128	W 310x143	45 °	90	45	90	60 °
SSWP-C-T-20	W760x220	W690x240	45 °	90	45	90	0 °
SSWP-C-T-21	W760x434	W690x419	45 °	90	45	90	0 °
SSWP-C-T-22	W 200x100	W 250x140	45 °	90	45	90	0 °
SSWP-C-T-23	W 690x170	W 610x155	45 °	90	45	90	0 °

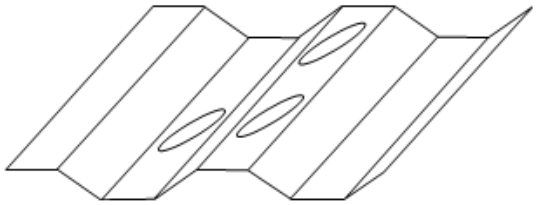

Figure 5 local buckling forms in trapezoidal corrugated plates

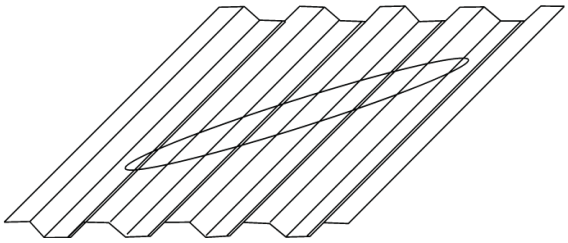

Figure 6 Global buckling forms in trapezoidal corrugated plates

Plate buckling failure may occur as local, global or interactive buckling. This failure depends on the configuration of the infill plate and plate thickness. For small plate thickness, the local buckling mode occurs due to weak resistance of out of plane deformation. In this paper plate thickness to wavelength ratio is lower than 1:120 which always buckles locally only and for ratio more than this, the buckling may be local, global or interactive. It is observed that for thicknesses more than 2 mm (4, 6, 7 and 9 mm) only the global buckling occurs. Regarding corrugation internal angle (α), for 15^0 angle only local buckling occurs for the tested thicknesses as the inclined part of corrugation which acts as a stiffener for plate in the out of plane direction has a small stiffness in the out of plane direction. For sinusoidal corrugated infill plate both local and global buckling occurs. First, the local buckling occurs in one corrugation wave

then developed-with the load increment- to global buckling see figures 7 and 8 respectively.

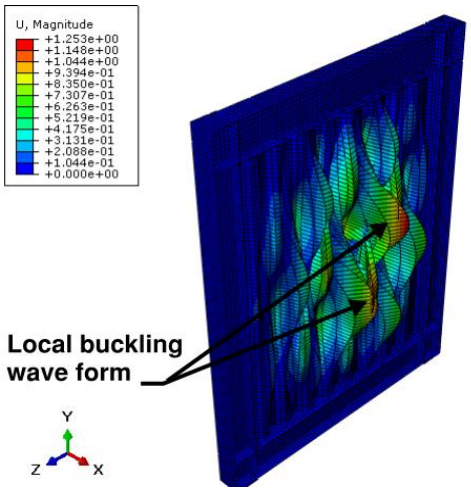

Figure 7 Trapezoidal corrugated plate local buckling

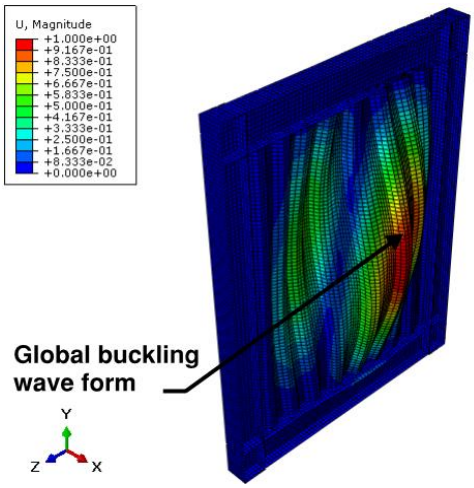

Figure 8 Trapezoidal corrugated plate global buckling

4.2. Boundary frame failure

Shear wall failure may occur as shear failure; in this case the boundary frame may fail due to either shear failure or buckling of the VBE. This pattern of failure, as shown in figure 9, collapses suddenly (shear failure mechanism). As per AISC Design Guide 20 [14], the limitation of boundary frame failure that would cause a plate failure not frame failure are as given in equations (16) and (17) respectively. Δt_p is difference in thickness of the infill plate between two stories.

Boundary frame failure depends not only on the corrugated plate orientation and infill plate thickness, but also on the dimensions and on properties of VBE and HBE. Regarding infill plate orientation, figure 10 shows specimen failure due to both frame failure and plate buckling failure.

$$I_{VBE} \geq 0.00307 \frac{t_p h^4}{L} \quad (16)$$

$$I_{HBE} \geq 0.003 \frac{(\Delta t_p) L^4}{H} \quad (17)$$

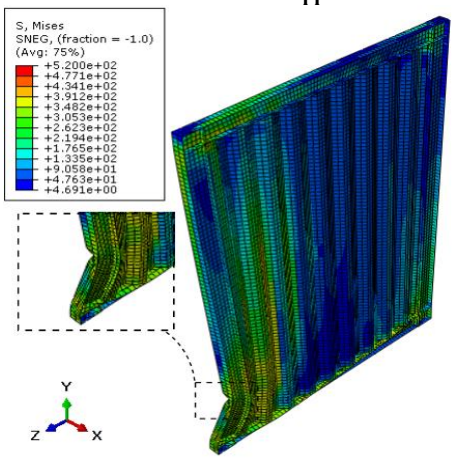

Figure 9 Shear failure for group – SSWP-C-T-2

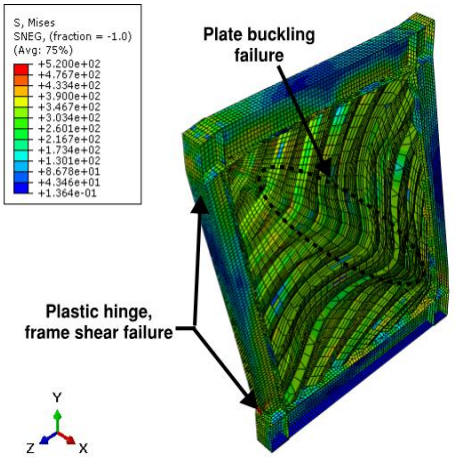

Figure 10 Shear and buckling failure for group-SSWP-C-T-9

For inclined corrugated infill plate specimens, the plate failure depends mainly on loading direction due to corrugated plate accordion action. Berman [9]; specified that the diagonal tension field action occurs only when the load is in the corrugation direction and the accordion action occurs when reversing the loading direction. Simply, two opposites in orientation (45^o and 135^o for example) shear walls can solve this problem. The case of load in an opposite direction regarding the corrugation direction (case of accordion failure) gives more capacity (about 30% for $\Theta = 45^o$) due to the high ductility of the shear wall in this case.

4.3. FEM analysis of corrugated plate shear wall geometrical properties.

The finite element model is used to conduct a parametric study for the trapezoidal and sinusoidal corrugated infill plate shear wall. Five parameters were chosen in this study, boundary frame properties (the plastic section modulus for both VBE Z_{VBE} and HBE Z_{HBE}), infill plate thickness (t_p), trapezoidal corrugation inclined angle (α), infill plate orientation (Θ degree) measured with vertical and corrugation dimensions (trapezoidal corrugation flat part length, corrugated plate depth and corrugation wave length).

4.3.1. Effect of infill plate corrugation orientation

Corrugated plate orientation angle (Θ^o) affects directly the shear wall capacity. For sinusoidal corrugated infill plate, only vertical and horizontal groups were tested in this paper. Vertically corrugated panels showed average resistance value of 1.18 of the horizontally corrugated panels and the vertically corrugated panels has higher stiffness by 6%.

The boundary frame and infill plate interact together in the shear wall, where the loads are transmitted from the boundary frame to the infill plate (see figure 11). The vertical corrugation configuration acts more efficiently and adequately rather than horizontal corrugation in interaction with the boundary frame elements. This may change depending on the shear wall height and width. The resultant axial shear force that resulted from the interaction is mainly a factor of the coupling, which is the resultant of the applied force. For vertical corrugation configuration, the deformed shape, as shown in figure 12, illustrates that the corrugation will be used in its proper direction, stiffening the wall out of plane stability.

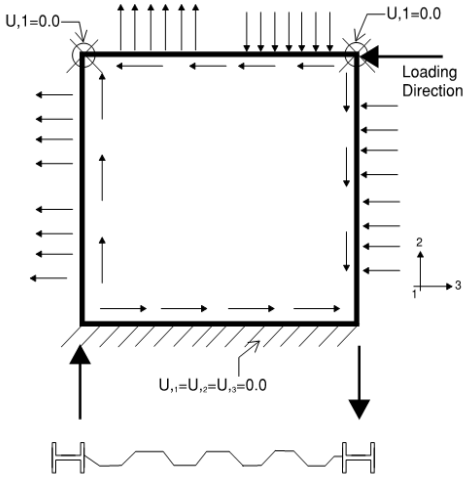

Figure 11 Frame and plate interaction due to lateral load

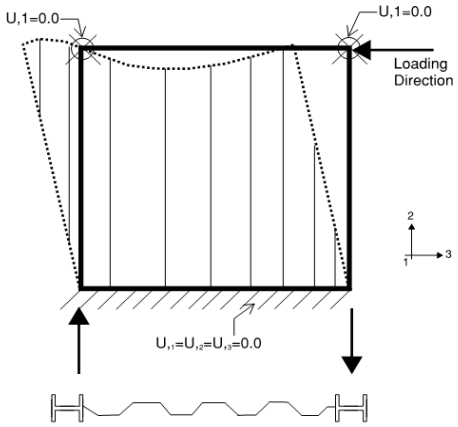

Figure 12 Shear wall deformed shape due to lateral load

Figure 13 shows the deformation of finite element model using the horizontal corrugation profile. For the other orientation angles of the infill plate, the same failure mechanism is observed besides the effect of accordion phenomena as mentioned before. Regarding trapezoidal corrugated infill plate, vertical corrugated has the highest value for the shear base force followed by corrugation orientation angles 30^o and 60^o respectively. Finally, the 45^o and 90^o have the lowest resistance. With the increase of t_p/L value (for thick plate with t_p/L_c more than 15/1000) it is observed that the ratio between horizontal corrugated shear wall capacity/flat shear wall capacity is higher than the ratio between vertical/flat one. Refer to figure 14 for the load-displacement curve sample for specimen group (SSWP-C-T-3) which shows the effect of infill plate thickness to wave length effect. This is because of the change in shear wall behavior and failure mechanism to flexure failure. The failure load remains constant whereas the displacement increases. Due to high ductility of horizontal corrugated shear wall in the load direction, the load capacity increases. For vertical corrugated shear wall, it gives much higher stiffness than the horizontal, so that failure occurs at early stage, which may not serve well in the serviceability case.

Figure 15 shows the relation between ultimate shear resistance of the shear wall and the thickness of the corrugated infill plate for different shear wall orientation Θ measured with vertical. It is clear that increasing infill plate to wavelength ratio (t_p/s) will increase shear force capacity of the shear wall.

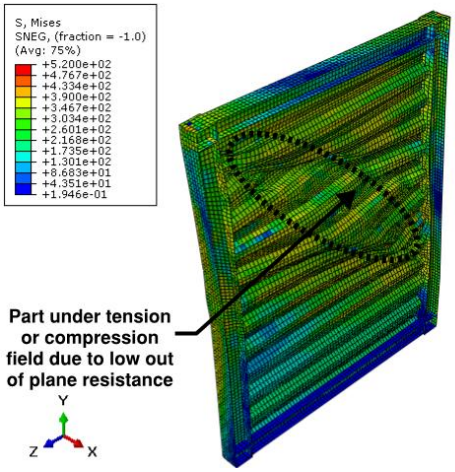

Figure 13 Horizontal corrugation configuration failure mechanism

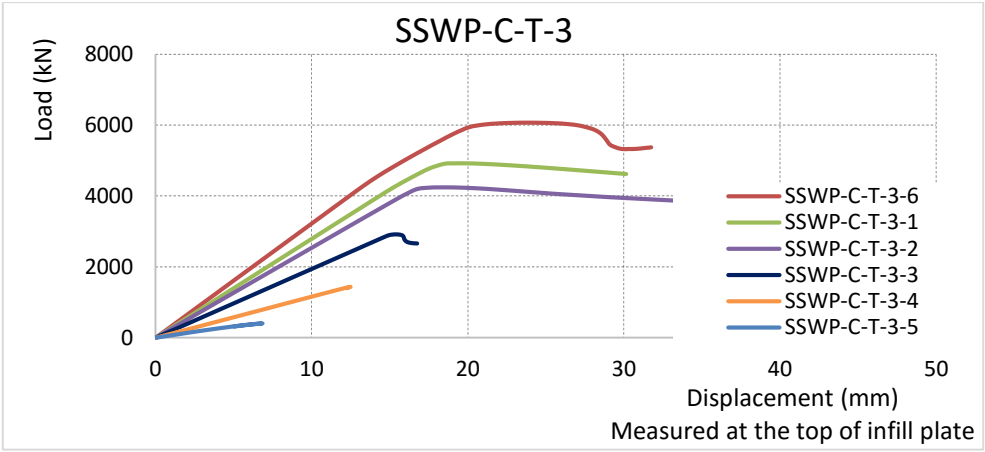

Figure 14 (P-Δ) Curve for sample for specimen group (SSWP-C-T-3)

Table 3 gives shear force values of the FE models for trapezoidal corrugated shear walls in different angels. All factors are assumed constant except "t_p/s" so all the following equation (18) will be used. $\tau_{equation}$ is the interactive buckling shear stress (τ_I) that is considered in equation (19) as reported by Heroshi et al. [15], where τ_{crl} is as per equation (5), τ_{crG} is as per equation (6) and τ_{FE} is the buckling shear stress obtained from the finite elements models.

Θ	**t_p/s (x10^2)**					
(Deg.)	**2.9**	**2.3**	**2.0**	**1.3**	**0.7**	**0.3**
0	6066	4916	4239	2916	1433	399
30	4194	3629	3163	2195	1157	503
45	3359	2743	2451	1839	1083	480
60	3130	2601	2342	1807	1062	481
90	5906	4791	4206	2896	1543	524

Table 3 Base shear reaction from FE models (kN)

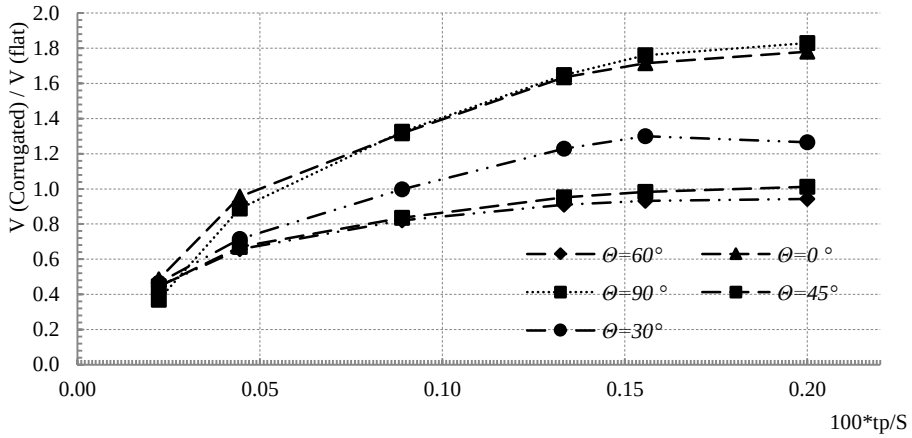

Figure 15 Base shear reactions for corrugated Vs flat shear walls and ($t_{p/S}$)

$$\frac{\tau_{FE}}{\tau_{equation}} = \delta = r\left(\frac{t_p}{s}\right)^n \quad (18)$$

$$\tau_I = \frac{1}{\left(\frac{1}{\tau_{crl}{}^4} + \frac{1}{\tau_{crG}{}^4}\right)^{1/4}} \quad (19)$$

Vertical corrugated shear wall gives the best performance. Values of r and n were calculated for each corrugation type and the best-estimated values are found as per equations (20) and (21).

$$r = 0.098 \sin \Theta^2 - 0.173 \sin \Theta + 0.092 \quad (20)$$

$$n = 0.396 \sin \Theta^2 - 0.650 \sin \Theta - 0.579 \quad (21)$$

These equations are developed to modify the corrugated plate buckling resistance in conjunction with the orientation of loading. r and n are considered as shear buckling stress modification factors.

4.3.2. Effect of corrugation dimensions:

Trapezoidal shear walls stiffness and buckling resistance is represented as corrugation dimension for a specific internal angel (α) or the total arc length to depth in the sinusoidal corrugated infill plates. The inclined part components, for both vertical and horizontal component, works as the shear wall support. Five different angles of corrugation are considered in this study as 15^0, 30^0, 45^0, 60^0 and 75^0 measured with horizontal as given in Table 4 respectively. For the 15^0 corrugated web inclination

angles, the plate is almost flat with low out-of-plane stiffness and the failure is similar to flat plate failure. Increasing the internal corrugation angle from 15° to 30° increases the total shear wall capacity by about 10% whereas from 30° to 45° increases the capacity by 15%. Above 45°, there is almost no buckling occurs in the shear wall due to corrugation high density and the shear failure occurs in the boundary frame or shear failure and crushing in the infill plate is dominant as seen in figures 16-a and 16-b respectively.

Figure 17 shows the relation between the corrugation internal angle effect and the resulted shear wall buckling strength using equation (18) and finite element results. Equation (22) presents the effect of internal angle as a function in the shear wall capacity.

The ratio L_c/S presents the number of waves that exists in the infill plate. Figure 18 shows the effect of changing the corrugation density (L_c/s) on the corrugated plate buckling capacity. Equation (23) gives the effect of corrugation density as a function of the total shear wall capacity.

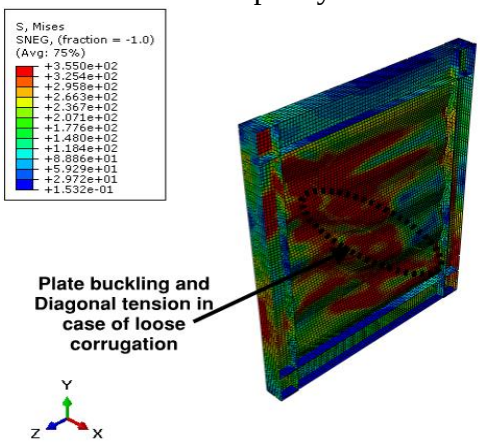

Figure 16-a Loose corrugation failure

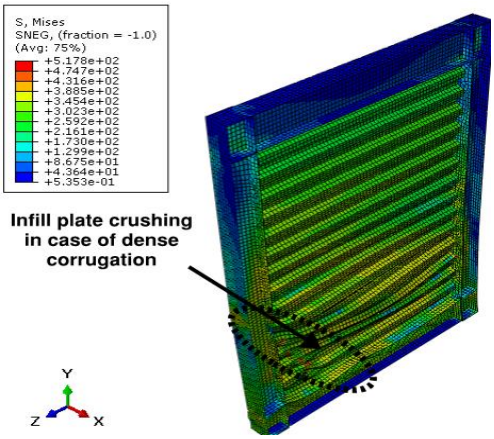

Figure 16-b Dense corrugation failure

Table 4 Shear stress modification factor m_1 calculated as per equation 18 and FEM results

Model	t_p (mm)	Corrugation data				τ_{eq18}	τ_{FEM}	m_1
		Deg. (α)	a (mm)	b (mm)	d (mm)			
C-T-0-13-2	6	15 °	340	45	90	339.1	170.7	0.5
C-T-0-14-2	6	30 °	155	45	90	271.2	167.4	0.62
C-T-0-3-2	6	45 °	90	45	90	239.6	151.7	0.63
C-T-0-15-2	6	60 °	50	45	90	223.8	138	0.62
C-T-0-16-2	6	75 °	25	45	90	217.2	115.6	0.53

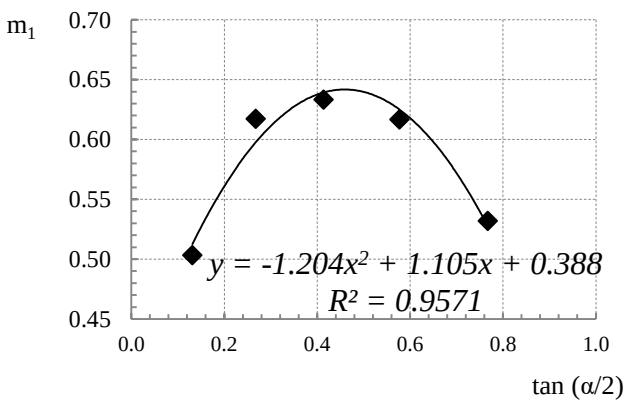

Figure 17 Relation between 'm_1' modification factor and tan (α/2)

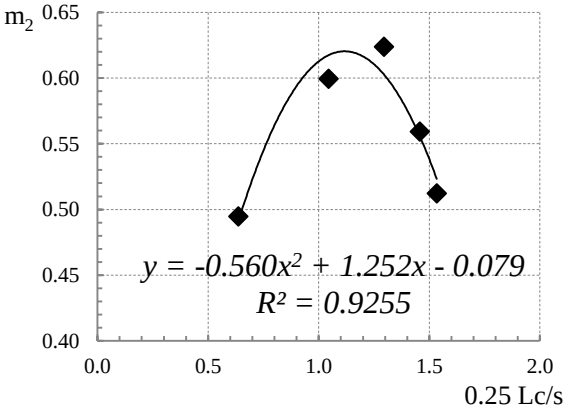

Figure 18 Relation between 'm_2' modification factor and $0.25L_c/S$

$m_1 = -1.204(\tan(\alpha/2))^2 + 1.105 \tan(\alpha/2) + 0.388$ (22)

$m_2 = -0.035 (L_c/s)^2 + 0.313(L_c/s) - 0.079$ (23)

The equations above are developed to explore (explane) the effect of corrugation density and corrugation angle effect on the corrugated infill plate buckling capacity of the shear walls, where m_1 and m_2 are modification factors as a function for the effect of corrugation dimensions on the total corrugated plate shear wall capacity.

4.3.3. Boundary frame properties effect:

Boundary frame is the main element distributing the lateral load to the infill plate. Properties of boundary frame are a major factor in governing the behavior of the shear wall and the failure mechanism. Figure 11 formally shows the boundary frame role in distributing the lateral load as indicated before. Group SSWP-C-T-2 shows pure shear failures in the VBE for all thicknesses. The shear failure occurs after corrugated plate elastic buckling occurs. Local distortion occurs in the lower horizontal boundary web despite stiffeners existing as per Figure 19. This failure is a very special case when infill plate thickness is 9 mm and boundary frame was W200x27 for beam and W250x39 for column. The cause of this failure is beam web crippling due to the axial load transformed from the infill plate in the VBE and lateral torsional buckling in the HBE, however that failure has not appeared in other groups due to high frame rigidity. Studies are executed in bare frame with the same boundary conditions and dimensions of the shear wall (see figure 24-a and 24-b). A pure shear behavior is observed, and the results coincide with the frame shear capacity equation.

In other groups, boundary frame affects directly the ultimate shear wall capacity. A new modification factor m_3 is introduced for different values of $\frac{Z_{HBE}+Z_{VBE}}{t_p{}^2 * L_c}$ as given in Table 5 and shown in Figure 21 to consider the effect of boundary frame element properties' on the shear wall buckling strength. Z_{HBE} and Z_{VBE} are the plastic moments of area for both beam and column respectively, and L_c is the corrugation length.

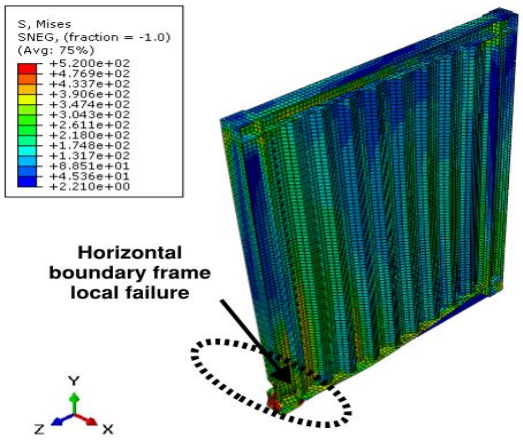

Figure 19 Boundary frame local failure

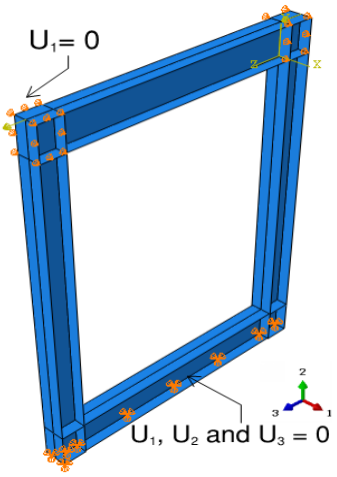

Figure 20-a Bare boundary frame layout and boundary condition

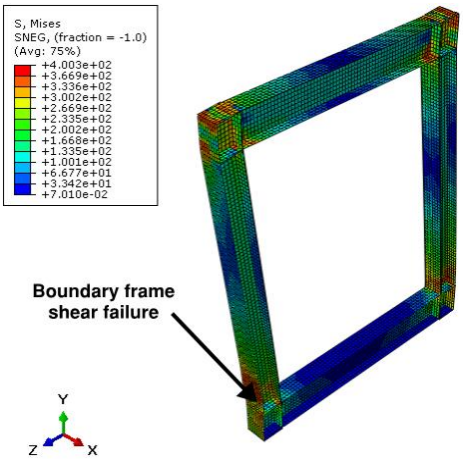

Figure 20-b Bare boundary frame shear failure

The shear wall failure changes from combined boundary frame shear and infill plate buckling behavior to infill plate buckling for $\frac{Z_{HBE}+Z_{VBE}}{t_p{}^2*L_c}$ ratio over 15. Equations (24-a) for $\frac{Z_{HBE}+Z_{VBE}}{t_p{}^2*L_c}$ less than 15 and equation (24-b) for $\frac{Z_{HBE}+Z_{VBE}}{t_p{}^2*L_c}$ more than 15 to present the effect of boundary frame. No reduced beams section was considered in this study.

$$m_3 = 0.04\left(\frac{Z_{HBE}+Z_{VBE}}{t_p{}^2*L_c}\right) + 0.3332 \text{ ---------- for } \left(\frac{Z_{HBE}+Z_{VBE}}{t_p{}^2*L_c}\right) \leq 15 \qquad (24\text{-a})$$

$$m_3 = 0.005\left(\frac{Z_{HBE}+Z_{VBE}}{t_p{}^2*L_c}\right)) + 0.828\text{----------} \text{ for } \left(\frac{Z_{HBE}+Z_{VBE}}{t_p{}^2*L_c}\right) > 15 \qquad (24\text{-b})$$

Where m_3 is modification factor as a function for the effect of boundary frame properties on the total corrugated plate shear wall capacity.

Table 5 shear stress modification factor m_3 calculated as per equation 18 and FEM results for Boundary frame.

Model No.	t_p (mm)	Corrugation data				τ_{eq18} (MPA)	τ_{FEM} (MPA)	m_3
		Deg. (α)	a (mm)	b (mm)	d (mm)			
SSWP-C-T-1	7	45 °	90	45	90	136.2	62.1	0.5
SSWP-C-T-2	7	45 °	90	45	90	136.2	115.7	0.8
SSWP-C-T-3	7	45 °	90	45	90	150.8	147	1
SSWP-C-T-20-1	7	45 °	90	45	90	175.9	202.4	1.2
SSWP-C-T-21-1	7	45 °	90	45	90	175.9	283.5	1.6
SSWP-C-T-22-1	7	45 °	90	45	90	137	123.3	0.9
SSWP-C-T-23-1	7	45 °	90	45	90	165.2	181.7	1.1

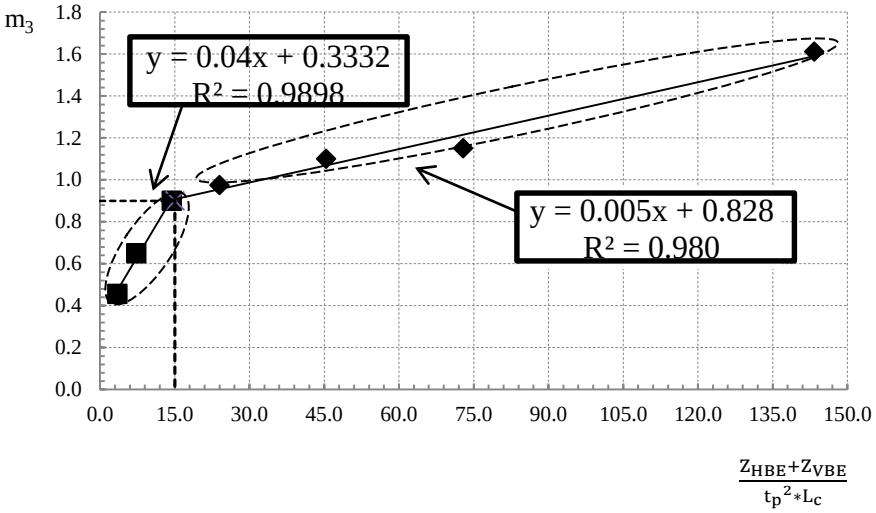

Figure 21 Equation 18 modification factor for the boundary frame properties

5- Suggested equation verification

Equation (25) gives the final modified equation with all parameters mentioned formerly in this paper.

$$\tau = (m_1 . m_2 . m_3) \frac{r\left(\frac{t_p}{s}\right)^n}{\left(\frac{1}{[K_l . \tau_l]^4} + \frac{1}{[K_g . \tau_g]^4}\right)^{1/4}} \quad (25)$$

This equation is verified with the finite element results with an acceptable deviation of 7.5%. Some limitations are restricted to the given equation (25) to be applicable and to give an acceptable result. These limitations such that; -

Ratio between infill plate thickness (t_p) and corrugated plate wavelength (s) should exceed 1/120 as beyond this limit the failure is due to boundary frame shear failure. Internal corrugation angle α should be between 35° and 55°.

Corrugation orientation should have an inclination angle Θ between 0° to 25° or 75° to 90° measured with vertical direction. For corrugation wavelength to corrugation total length (corrugation density) $0.25L_c/s$ this ratio applied between 0.85 and 1.25.

Figure 22 shows the comparison between results from equation (25) and FEM results for the five groups with the vertical corrugations and for infill plate thickness = 7 mm. Figures 23 and 24 shows a comparison between critical shear stress resulting from equation (25) and the shear yield stress $\tau_y = \frac{F_y}{\sqrt{3}}$ for different corrugation angles.

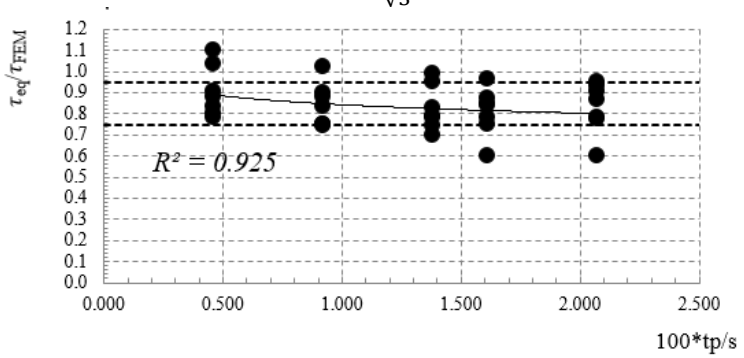

Figure 22 Comparison between the buckling stress from FE models and equation 25

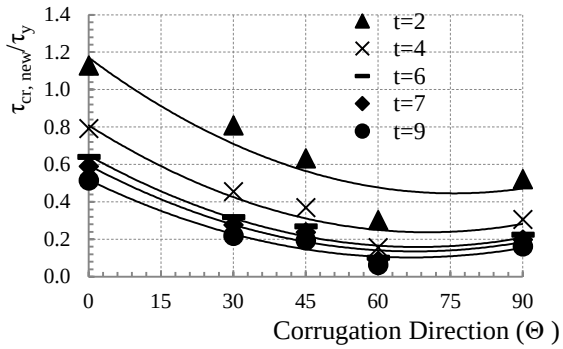

Figure 23 Comparison between the buckling stress from FE models and shear yield stress regarding infill plate orientation

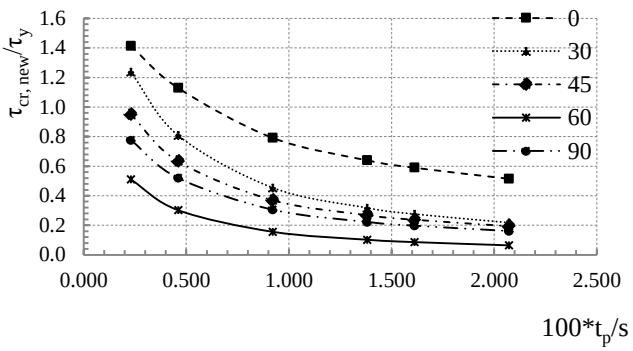

Figure 24 Comparison between the buckling stress from FE models and Shear yield stress regarding infill t/s value

6- Conclusions and recommendations

This study investigates the ultimate bearing capacity of shear walls with corrugated plates. The study includes the effect of different geometrical parameters on the corrugated plate capacity. Different parameters studied are considered mainly for the vertically oriented corrugation shear walls and other are used for comparison as the following results obtained:

Increasing the infill plate thickness in all types of infill plates (flat, trapezoidal and sinusoidal), will increase ultimate capacity and stiffness of the shear wall. In general, corrugated plate shear wall has much more stiffness than flat plate shear wall. Plate buckling occurs in the corrugated plate in most of the cases but the failure mechanism changes depending on the dimensions and properties of the shear wall.

Using vertically corrugated infill plate with corrugated plate wavelength more than 120 times infill plate thickness gives shear capacity almost twice of the flat plate shear wall capacity. For higher values, this ratio drops to 1.18. Moreover, vertically corrugated panels has stiffness much more than horizontal one by 6%.

Using inclined corrugation with 60^o corrugated infill gives shear capacity equals to 1.2 the flat plate shear wall.

Vertically corrugated sinusoidal shear wall gives resultant value in shear capacity equals to 1.7 the flat plate shear wall.

Using corrugated plate with corrugation density (wavelength to total corrugation length) more than 1:5 (very dense corrugation) decreases the total shear wall capacity due to plate sudden failure.

Infill plate failure occurs due to global buckling failure if the ratio between plate thickness and wavelength is more than 1:120; otherwise local buckling occurs and the failure is shear failure in the boundary frame.

When tp/L value increases (12.5/10000), the horizontal corrugated shear wall capacity/flat shear wall capacity is more than the vertical/flat one, this is because of the change in shear wall behavior and failure mechanism to flexure failure (failure load is constant and the displacement increases).

Increasing the internal corrugation angle from 15 to 30 increases the shear reaction with about 10% and from 30 to 45 with about 15%.

7- References

[1] Thorburn, L. J., Kulak, G. L., and Montgomery, C. J., (1983), "Analysis of Steel Plate shear Walls", Structural Engineering Report 107, Department of Civil and environmental Engineering, University of Alberta, Edmonton, Alberta, 152pp.

[2] Timler, P. A. and Kulak, G. L., (1983), "Experimental Study of Steel Plate Shear Walls", Structural Engineering Report 114, Department of Civil and Environmental Engineering, University of Alberta, Edmonton, Alberta, 101pp.

[3] Berman, J., and Bruneau, M., (2003a), "Plastic Analysis and Design of Steel Plate Shear Walls," Journal of Structural Engineering, ASCE, Vol. 129 No. 11, February, pp. 1448-1456.

[4] B.Qu,M.Bruneau, Seismic behavior and design of boundary frame members of steel plate shear wall, Technical report MCEER-08-0012. Multidisciplinary (2009).

[5] Jalali A., Sazgari A. 2006. \Experimental and Theoretical Post-Buckling Study of SteelShear Walls". Proceedings of the 4th International Conference on Earthquake Engineering Paper No. 114.

[6] Elgaaly, M., Smith, D., and Hamilton, R., (1992), "Beams and Girders with Corrugated Webs," NSF Structures, Geomechanics, and Buildings System Grantees Conference, Proceedings, San Juan, Puerto Rico, June, pp. 126-128.

[7] Elgaaly, M., Caccese, V., and Du, C., (1993), "Post Buckling Behaviour of Steel Plate Shear Walls under Cyclic Loads," Journal of Structural Engineering, ASCE, Vol. 119, No. 2, February, pp. 588-605.

[8] Elgaaly, M., Seshadri, A., and Hamilton, R., (1995), "Beams with Corrugated Webs, Research to Practice," Research Transformed into Practice: Implementation of NSF Research, Proceedings, Conference sponsored by National Science Foundation, Arlington, Virginia, June, pp. 601-612.

[9] Berman, J., and Bruneau, M., (2005), "Experimental Investigation of Light-Gauge Steel Plate Shear Walls," Journal of Structural Engineering, ASCE, Vol. 131 No. 2, February, pp. 259-267.

[10] G. Kiymaz, E. Coskun, C. Cosgun, and E. Seckin, "Transverse load carrying capacity of sinusoidally corrugated steel web beams with web openings," Steel and Composite Structures, vol. 10, no. 1, pp. 69–85, (2010).

[11] Emami, F., Mofid, M., Vafai, A. (2013). Experimental study on cyclic behavior of trapezoidally corrugated steel shear walls. Engineering Structures 48:750-762.

[12] Analysis User's Manual, Volume II: Analysis. Dassault Systems Simulia Corp. Abaqus 6.10, USA, 2010.

[13] CISC Handbook of Steel Construction [Canadian Institute of Steel Construction].

[14] Sabelli, R., and Bruneau, M. (2007). "Steel plate shear walls." AISC Steel Design Guide 20, American Institute of Steel Construction,Chicago.

[15] Hiroshi Shiratoni, Hiroyuki Ikeda, Yohiaki Imai, KoichiKano. Flexural shear behavior of composite bridge girder with corrugated steel web's around middle support. JSCEJ 2003;724(I-62):4967.